



Research paper

Thiophenol-formaldehyde triazole causes apoptosis induction in ovary cancer cells and prevents tumor growth formation in mice model



Yan Jia ^a, Lihui Si ^a, Ruixin Lin ^b, Hongjuan Jin ^c, Wenwen Jian ^a, Qing Yu ^a, Shuli Yang ^{a,*}

^a Department of Gynaecology and Obstetrics, The Second Hospital of Jilin University, Changchun, Jilin, 130041, China

^b Department of Hepatopancreatobiliary Surgery, The Second Hospital of Jilin University, Changchun, Jilin, 130041, China

^c Department of Plastic and Aesthetic Surgery, The First Hospital of Jilin University, Changchun, Jilin, 130021, China

ARTICLE INFO

Article history:

Received 2 January 2019

Received in revised form

13 March 2019

Accepted 14 March 2019

Available online 20 March 2019

Keywords:

Macrophages
Pharmacophore
Heterocyclic
Metastasis
Migration

ABSTRACT

In the present study a library of thiophenol-formaldehyde-triazole (TFT) derivatives was synthesized and screened against CAO3, CAO4 and ES-2 ovary cancer cell lines. Initial screening revealed that five-compounds **5a**, **5b**, **5j**, **5h** and **5i** inhibited the viability of tested cell lines. Analysis of apoptosis revealed that increase in compound **5a** (most active) concentration from 0.25 to 2.0 μM enhanced apoptotic cell proportion. Transwell assay showed reduction in invasive potential of CAO3 cells on treatment with compound **5a**. In wound healing assay increasing the concentration of compound **5a** from 0.5 to 2.0 μM caused a significant ($P < 0.05$) decrease in the migration potential. Western blotting showed that compound **5a** treatment markedly decreased the level of matrix metalloproteinase (MMP)-2 and -9 in CAO3 cells. Treatment of CAO3 cells with compound **5a** caused a marked decrease in Focal Adhesion Kinase (FAK) activation. Tumor growth was inhibited in the compound **5a** treated mice markedly than those of untreated group. The tumor metastasis to liver, intestine, spleen and peritoneal cavity was markedly decreased in mice treated with 10 mg/kg dose of compound **5a**. Examination of Von Willebrand factor (vWF) expression in liver, intestinal and pulmonary lesions showed a marked decrease in the compound **5a**-treated mice. The infiltration of macrophages in the metastatic lesions showed a significant decrease in compound **5a**-treated mice. In conclusion, the compound **5a** inhibited ovary cancer cell viability and induced apoptosis through decrease in expression of vWF and metalloproteinase, suppression of FAK activation and decrease in infiltration of macrophages. The compound **5a** therefore can be investigated further for the treatment of ovary cancer.

© 2019 Published by Elsevier Masson SAS.

1. Introduction

Ovarian cancer is the most common cause of mortality among gynaecologic cancers and the fifth leading cause of deaths in females because of cancer [1]. The 5-year survival rate of the females suffering from ovarian cancer is very low which stresses for the development of an effective treatment strategy for the ovary cancer [2]. Difficulty in the detection of ovary cancer at an early stage and dearth of available effective treatment makes ovary cancer a life-threatening disease in females [3]. In ovarian cancer patients tumor metastasis to the peritoneal tissues takes place at an advanced stage [4]. Inhibition of ovarian cancer growth and its metastasis to

the distant organs demands for the development of novel and effective treatment strategies. Studies are being continuously performed to investigate the mechanism of ovarian cancer for development of efficient treatment strategies [5–8].

Triazole moiety comprises of a heterocyclic aromatic five-membered ring and constitutes an important pharmacophore of several bioactive molecules (Fig. 1) [9]. The molecules containing triazole scaffold possess several biological activities like anti-tumor, anti-inflammatory, etc. [9]. A large number of compounds bearing triazole moiety have been identified as the biologically active molecules [10]. Screening of the 5-mercapto-1,2,4-triazole derivatives has led to the identification various molecules possessing anticancer activity against various types of carcinoma cell lines [11–13]. Molecular docking results demonstrate that 1,2,4-triazole compounds inhibit proliferation of cancer cells through apoptosis

* Corresponding author.

E-mail address: SusannPdgesc@yahoo.com (S. Yang).

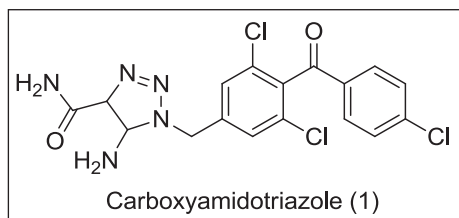


Fig. 1. Structure of triazole possessing anticancer activity.

induction by acting as inhibitors for methionine aminopeptidase type II [14]. The 1,2,4-triazole derivatives are synthesized and assessed for anti-cancer activity using docking simulation [15]. The *in vitro* screening of the triazole derivatives have shown significant activity against several types of cancer cells like ovarian, pulmonary and melanoma [15]. The triazole derivatives synthesized from various molecules also lead to the development of novel compounds possessing antimicrobial activity [16,17]. The present study was aimed to synthesize a series of thiophenol-formaldehyde triazoles (TFT) and to investigate the synthesized molecules against the ovary cancer cell lines. The study demonstrated that among the synthesized library compound **5a** is the most active against ovarian cancer cells. The effect of compound **5a** was also analysed on tumor metastasis in mice model of ovary cancer. The study demonstrated inhibition of ovary cancer cell viability through apoptosis induction and suppression of tumor metastasis in mice by down-regulation of vWF expression.

1,2,3-Triazole derivatives have been synthesized since long and explored mainly for their anti-tumor potential [18]. The 2-methoxy-5-(1-(3,4,5-trimethoxyphenyl)-1H-1,2,3-triazol-5-yl)aniline have been shown to inhibit tubulin polymerization through interaction with β -tubulin via H-bonding with the amino acids [19]. Another compound, 3-(4-(4-phenoxyphenyl)-1H-1,2,3-triazol-1-yl)benzo [d]isoxazole was found to significantly inhibit the proliferation of MV4-11 cells at an IC_{50} of 2 μ M [20]. The 4-[phenyl-1-(1-phenyl-ethyl)]-1H-1,2,3-triazole displayed promising cytotoxic activity against HL 60 cells [21]. The preparation of 1,2,3-triazole derivatives of flavonoid, quinolone and oxadiazole lead to the identification of compounds which inhibit growth of leukemia K-562 and melanoma SK-MEL-5 cell lines [22]. The 1,2,3-triazole derivatization of betulinic acid lead to the identification of two compounds, 3{1N(2-cyanophenyl)-1H1,2,3-triazol-4yl}methoxy betulinic acid and 3{1N(5-hydroxy-naphth-1yl)-1H-1,2,3-triazol-4yl}methoxy betulinic acid with significant anti-proliferation activity against leukemia cells HL-60 [23].

2. Materials and methods

2.1. Chemistry

2.1.1. General

1H and ^{13}C NMR spectra of all the triazoles synthesized was recorded in $(CD_3)_2SO$ solvent using a Bruker AC-300P spectrometer. The tetramethylsilane (TMS) was used as the internal standard. The values of chemical shift (δ values) and coupling constants (J values) are presented in ppm and Hz, respectively. The Bruker Daltonics electro spray ionization apparatus was used for the measurement of HRMS of all the compounds synthesized. Thin layer chromatography was performed using commercially available silica gel plates GF254 aluminium plates. The chemicals used for experiments and solvents were obtained from Sigma-Aldrich (Sigma, St. Louis, MO, USA). Purification of the compounds was achieved using column chromatography on silica gel (Qualigens, 60–120 mesh).

2.1.2. General procedure for propargylation

The solution of compound **3** (500 mg, 1.0 mmol) in THF was stirred with NaH (600 mg, 1.0 mmol) and propargyl bromide (458 μ L, 4.0 mmol) for 1 h at room temperature. The completion of the reaction was monitored by TLC. After 1 h, the reaction mixture was purified by the column chromatography using 2:98 ethyl acetate/hexane as the solvent system.

2.1.3. Procedure for preparation of azides

Aromatic Azides. To a solution of 2,5-dimethyl aniline (500 mg, 4.13 mmol) in 1,4-dioxane at $-15^\circ C$, 2 M sulphuric acid (10.3 mL, 20.6 mmol) was added in small instalments while stirring [24]. After 5 min, 3 M aqueous sodium nitrite solution (2.75 mL, 8.26 mmol) was added drop wise followed by careful addition of 3 M sodium azide solution (4.13 mL, 12.39 mmol). After the addition was over, the reaction mixture was allowed to attain room temperature and extracted with diethyl ether (3×50 mL). The combined organic layer was washed with saturated sodium bicarbonate solution, dried over anhydrous sodium sulfate, and concentrated under reduced pressure to yield aromatic azide that was used in the next reaction without purification.

Aliphatic Azides. A mixture of octanol (4.6 mL, 3.8 mmol), triphenylphosphine (1.2 g, 4.6 mmol), iodine (1.16 g, 4.6 mmol), and imidazole (0.26 g, 3.84 mmol) was thoroughly mixed in a round bottom flask [24]. To this mixture was added sodium azide (0.99 g, 15.3 mmol) in DMSO and stirred at room temperature for 1 h. The reaction mixture was extracted with diethyl ether (3×30 mL), washed with brine, and concentrated under reduced pressure to yield crude aliphatic azide that was used in the next reaction without further purification.

2.1.4. General procedure for synthesis of triazole compounds (5a–5u)

The compound **4** (300 mg, 1.0 mmol) was dissolved in 5 ml of $H_2O: tBuOH$ (2:1) mixture. To this solution was added $CuSO_4$ (20 mol%) and alkyl or aryl azide (1.5 mmol) and the mixture was subjected to sonication at $45^\circ C$ for 1–2 h. The progress of the reaction was monitored by TLC. The products obtained were characterized by 1H NMR, ^{13}C NMR, and HRMS techniques; 2-(((1-(2-fluorophenyl)-1H-1,2,3-triazol-4-yl)methoxy)methyl)benzenethiol (**5a**). 1H NMR (400 MHz, $(CD_3)_2SO$) δ 8.01 (1H, s), 7.53–7.55 (1H, m), 7.20 (1H, d, $J = 8.0$ Hz), 7.12–7.03 (6H, m), 4.68 (2H, s), 4.66 (2H, s), 4.24 (1H, s); ^{13}C NMR (101 MHz, $(CD_3)_2SO$) δ 159.57, 157.47, 151.99, 133.75, 130.12, 128.05, 127.96, 127.54, 125.75, 125.70, 122.06, 122.02, 118.01, 117.80, 70.59, 60.04; HRMS (ESI) m/z calcd. for $C_{16}H_{14}FN_3OS$ $[M]^+$: 315.0842, found: 315.0842; yield: 89%; melting point: 203–205 $^\circ C$.

2-(((1-(2,4-difluorophenyl)-1H-1,2,3-triazol-4-yl)methoxy)methyl)benzenethiol (**5b**). 1H NMR (400 MHz, $(CD_3)_2SO$) δ 8.03 (1H, s), 7.58–7.54 (1H, m), 7.21–7.19 (1H, m), 7.09–7.01 (4H, m), 6.91–6.83 (1H, m), 4.68 (2H, s), 4.66 (2H, s), 3.29 (1H, s); ^{13}C NMR (101 MHz, $(CD_3)_2SO$) δ 161.80, 160.27, 159.70, 151.99, 133.75, 130.12, 129.54, 127.96, 123.19, 122.98, 114.69, 114.66, 105.95, 105.52, 70.59, 60.04; HRMS (ESI) m/z calcd. for $C_{16}H_{13}F_2N_3OS$ $[M]^+$: 333.0747, found: 333.0747; yield: 92%; melting point: 206–209 $^\circ C$.

2-(((1-(4-bromophenyl)-1H-1,2,3-triazol-4-yl)methoxy)methyl)benzenethiol (**5c**). 1H NMR (400 MHz, $(CD_3)_2SO$) δ 8.03 (1H, s), 7.43 (2H, d, $J = 8.0$ Hz), 7.25 (2H, d, $J = 8.0$ Hz), 7.19–7.02 (4H, m), 4.66 (4H, s), 3.15 (1H, s); ^{13}C NMR (101 MHz, $(CD_3)_2SO$) δ 151.53, 135.45, 133.75, 132.19, 130.12, 129.54, 127.96, 127.27, 127.07, 121.80, 121.05, 120.54, 70.59, 60.04; HRMS (ESI) m/z calcd. for $C_{16}H_{14}BrN_3OS$ $[M]^+$: 375.0041, found: 375.0041; yield: 90%; melting point: 204–206 $^\circ C$.

2-(((1-(2-bromophenyl)-1H-1,2,3-triazol-4-yl)methoxy)methyl)benzenethiol (**5d**). 1H NMR (400 MHz, $(CD_3)_2SO$) δ 8.03 (1H, s), 7.48–7.46 (2H, m), 7.22–6.99 (6H, m), 6.65 (4H, s), 4.66 (4H, s), 4.17

(1H, s); ^{13}C NMR (101 MHz, $(\text{CD}_3)_2\text{SO}$) δ 151.99, 137.93, 133.75, 133.34, 132.10, 130.12, 129.54, 129.03, 127.96, 127.27, 127.07, 126.24, 124.71, 122.03, 121.05, 114.90, 70.59, 60.04; HRMS (ESI) m/z calcd. for $\text{C}_{16}\text{H}_{14}\text{BrN}_3\text{OS}$ $[\text{M}]^+$: 375.0041, found: 375.0041; yield: 92%; melting point: 212 °C.

2-(((1-(3-bromophenyl)-1H-1,2,3-triazol-4-yl)methoxy)methyl)benzenethiol (**5e**). ^1H NMR (400 MHz, $(\text{CD}_3)_2\text{SO}$) δ 8.03 (1H, s), 7.81 (1H, s), 7.45–7.47 (1H, m), 7.23–7.02 (6H, m), 4.69 (2H, s), 4.65 (2H, s), 3.28 (1H, s); ^{13}C NMR (101 MHz, $(\text{CD}_3)_2\text{SO}$) δ 151.53, 139.27, 133.75, 130.50, 130.12, 129.54, 128.07, 127.96, 127.27, 127.07, 122.91, 122.86, 121.05, 118.29, 70.59, 60.04; HRMS (ESI) m/z calcd. for $\text{C}_{16}\text{H}_{14}\text{BrN}_3\text{OS}$ $[\text{M}]^+$: 375.0041, found: 375.0041; yield: 88%; melting point: 217 °C.

2-(((1-(4-chlorophenyl)-1H-1,2,3-triazol-4-yl)methoxy)methyl)benzenethiol (**5f**). ^1H NMR (400 MHz, $(\text{CD}_3)_2\text{SO}$) δ 8.03 (1H, s), 7.32 (2H, d, $J = 8.0$ Hz), 7.26 (2H, d, $J = 8.0$ Hz), 7.19–7.02 (4H, m), 4.66 (4H, s), 4.15 (1H, s); ^{13}C NMR (101 MHz, $(\text{CD}_3)_2\text{SO}$) δ 151.53, 136.01, 133.75, 132.65, 130.12, 129.54, 129.01, 127.96, 127.27, 127.07, 122.93, 121.05, 70.59, 60.04; HRMS (ESI) m/z calcd. for $\text{C}_{16}\text{H}_{14}\text{ClN}_3\text{OS}$ $[\text{M}]^+$: 331.0546, found: 331.0546; yield: 90%; melting point: 206–209 °C.

2-(((1-(3,4-dimethylphenyl)-1H-1,2,3-triazol-4-yl)methoxy)methyl)benzenethiol (**5g**). ^1H NMR (400 MHz, $(\text{CD}_3)_2\text{SO}$) δ 8.03 (1H, s), 7.40 (1H, s), 7.28–7.02 (6H, m), 4.69 (2H, s), 4.65 (2H, s), 3.28 (1H, s), 2.35 (3H, s), 2.33 (3H, s); ^{13}C NMR (101 MHz, $(\text{CD}_3)_2\text{SO}$) δ 151.53, 140.54, 138.13, 134.35, 133.75, 132.06, 130.12, 129.54, 127.96, 127.27, 127.07, 126.12, 125.44, 121.05, 70.59, 60.04, 20.37, 19.44; HRMS (ESI) m/z calcd. for $\text{C}_{18}\text{H}_{19}\text{N}_3\text{OS}$ $[\text{M}]^+$: 325.1249, found: 325.1249; yield: 86%; melting point: 218 °C.

2-(((1-(2-(trifluoromethyl)phenyl)-1H-1,2,3-triazol-4-yl)methoxy)methyl)benzenethiol (**5h**). ^1H NMR (400 MHz, $(\text{CD}_3)_2\text{SO}$) δ 8.03 (1H, s), 7.91–7.80 (2H, m), 7.48 (1H, m), 7.28–7.05 (5H, m), 4.65 (4H, s), 3.15 (1H, s); ^{13}C NMR (101 MHz, $(\text{CD}_3)_2\text{SO}$) δ 151.99, 136.03, 135.98, 132.86, 130.12, 129.54, 128.94, 127.96, 127.27, 127.21, 127.14, 126.85, 124.75, 122.03, 121.12, 70.59, 60.04; HRMS (ESI) m/z calcd. for $\text{C}_{17}\text{H}_{14}\text{F}_3\text{N}_3\text{OS}$ $[\text{M}]^+$: 365.0810, found: 365.0810; yield: 89%; melting point: 207–208 °C.

2-(((1-(4-(trifluoromethyl)phenyl)-1H-1,2,3-triazol-4-yl)methoxy)methyl)benzenethiol (**5i**). ^1H NMR (400 MHz, $(\text{CD}_3)_2\text{SO}$) δ 8.03 (1H, s), 7.75 (2H, d, $J = 8.0$ Hz), 7.66 (2H, d, $J = 8.0$ Hz), 7.64–7.05 (4H, m), 4.65 (2H, s), 4.56 (2H, s), 3.40 (1H, s); ^{13}C NMR (101 MHz, $(\text{CD}_3)_2\text{SO}$) δ 151.53, 142.39, 133.75, 130.12, 129.54, 127.96, 126.91, 125.51, 123.81, 121.76, 121.70, 121.64, 121.59, 121.32, 121.05, 70.59, 60.04; HRMS (ESI) m/z calcd. for $\text{C}_{17}\text{H}_{14}\text{F}_3\text{N}_3\text{OS}$ $[\text{M}]^+$: 365.0810, found: 365.0810; yield: 91%; melting point: 209 °C.

2-(((1-(2,4,6-trichlorophenyl)-1H-1,2,3-triazol-4-yl)methoxy)methyl)benzenethiol (**5j**). ^1H NMR (400 MHz, $(\text{CD}_3)_2\text{SO}$) δ 8.03 (1H, s), 7.43 (2H, s), 7.21–7.19 (1H, m), 7.08–7.01 (3H, m), 4.70 (2H, s), 4.65 (2H, s), 3.29 (1H, s); ^{13}C NMR (101 MHz, $(\text{CD}_3)_2\text{SO}$) δ 150.75, 138.70, 135.84, 135.10, 133.75, 130.12, 129.85, 129.54, 127.96, 127.27, 127.07, 119.63, 70.59, 60.04; HRMS (ESI) m/z calcd. for $\text{C}_{16}\text{H}_{12}\text{Cl}_3\text{N}_3\text{OS}$ $[\text{M}]^+$: 398.9767, found: 398.9767; yield: 92%; melting point 206 °C.

2-(((1-(naphthalen-1-yl)-1H-1,2,3-triazol-4-yl)methoxy)methyl)benzenethiol (**5k**). ^1H NMR (400 MHz, $(\text{CD}_3)_2\text{SO}$) δ 8.28 (1H, d, $J = 4.0$ Hz), 8.03 (1H, s), 8.50–8.52 (1H, m), 7.62–7.01 (9H, m), 4.72 (2H, s), 4.66 (2H, s), 3.31 (1H, s); ^{13}C NMR (101 MHz, $(\text{CD}_3)_2\text{SO}$) δ 150.80, 136.80, 134.10, 133.75, 130.12, 129.54, 128.31, 127.96, 127.29, 127.28, 127.07, 126.86, 126.40, 125.69, 124.22, 123.60, 122.06, 112.84, 70.59, 60.04; HRMS (ESI) m/z calcd. for $\text{C}_{20}\text{H}_{17}\text{N}_3\text{OS}$ $[\text{M}]^+$: 347.1092, found: 347.1092; yield: 90%; melting point: 219 °C.

2-(((1-phenyl)-1H-1,2,3-triazol-4-yl)methoxy)methyl)benzenethiol (**5l**). ^1H NMR (400 MHz, $(\text{CD}_3)_2\text{SO}$) δ 8.03 (1H, s), 7.35–7.37 (2H, m), 7.21–6.93 (7H, m), 4.66 (4H, s), 34.13 (1H, s); ^{13}C NMR (101 MHz, $(\text{CD}_3)_2\text{SO}$) δ 151.53, 137.08, 133.75, 130.12, 129.54, 129.27, 127.96, 127.60, 127.27, 127.07, 121.38, 121.05, 70.59, 60.04; HRMS

(ESI) m/z calcd. for $\text{C}_{16}\text{H}_{15}\text{N}_3\text{OS}$ $[\text{M}]^+$: 297.0936, found: 297.0936; yield: 88%; melting point: 212–214 °C.

2-(((1-(*m*-tolyl)-1H-1,2,3-triazol-4-yl)methoxy)methyl)benzenethiol (**5m**). ^1H NMR (400 MHz, $(\text{CD}_3)_2\text{SO}$) δ 8.03 (1H, s), 7.43 (1H, d, $J = 4.0$ Hz), 7.32–7.34 (1H, m), 7.23–6.88 (6H, m), 4.70 (2H, s), 4.65 (2H, s), 3.29 (1H, s), 2.35 (3H, s); ^{13}C NMR (101 MHz, $(\text{CD}_3)_2\text{SO}$) δ 151.53, 139.18, 138.72, 133.75, 130.12, 129.54, 128.41, 127.96, 127.27, 127.07, 126.49, 124.15, 121.05, 116.19, 70.59, 60.04, 21.20; HRMS (ESI) m/z calcd. for $\text{C}_{17}\text{H}_{17}\text{N}_3\text{OS}$ $[\text{M}]^+$: 311.1092, found: 311.1092; yield 86%; melting point 209–211 °C.

2-(((1-(2-nitrophenyl)-1H-1,2,3-triazol-4-yl)methoxy)methyl)benzenethiol (**5n**). ^1H NMR (400 MHz, $(\text{CD}_3)_2\text{SO}$) δ 8.03 (1H, s), 8.90–8.81 (2H, m), 7.53–7.40 (2H, m), 7.22–7.04 (4H, m), 4.69 (2H, s), 4.67 (2H, s), 4.01 (1H, s); ^{13}C NMR (101 MHz, $(\text{CD}_3)_2\text{SO}$) δ 151.99, 141.93, 133.75, 133.19, 132.74, 130.12, 129.54, 128.04, 128.01, 127.96, 127.27, 127.07, 126.18, 122.03, 70.59, 60.04; HRMS (ESI) m/z calcd. for $\text{C}_{16}\text{H}_{14}\text{N}_4\text{O}_3\text{S}$ $[\text{M}]^+$: 342.0787, found: 342.0787; yield 89%; melting point 203–205 °C.

2-(((1-(3-nitrophenyl)-1H-1,2,3-triazol-4-yl)methoxy)methyl)benzenethiol (**5o**). ^1H NMR (400 MHz, $(\text{CD}_3)_2\text{SO}$) δ 8.33 (1H, s), 8.03 (1H, s), 7.81.7.79 (1H, m), 7.52–7.50 (2H, m), 7.23–7.02 (4H, m), 4.70 (2H, s), 4.67 (2H, s), 3.29 (1H, s); ^{13}C NMR (101 MHz, $(\text{CD}_3)_2\text{SO}$) δ 151.53, 147.64, 137.68, 133.75, 131.09, 130.12, 129.54, 127.96, 127.27, 127.07, 126.18, 121.05, 119.90, 70.59, 60.04; HRMS (ESI) m/z calcd. for $\text{C}_{16}\text{H}_{14}\text{N}_4\text{O}_3\text{S}$ $[\text{M}]^+$: 342.0787, found: 342.0787; yield: 90%; melting point: 205–208 °C.

2-(((1-(2,4-dinitrophenyl)-1H-1,2,3-triazol-4-yl)methoxy)methyl)benzenethiol (**5p**). ^1H NMR (400 MHz, $(\text{CD}_3)_2\text{SO}$) δ 8.70 (1H, s), 8.30 (1H, d, $J = 8.0$ Hz), 8.12–8.03 (2H, m), 7.19–7.21 (2H, m), 7.07–7.05 (2H, m), 4.70 (2H, s), 4.67 (2H, s), 4.01 (1H, s); ^{13}C NMR (101 MHz, $(\text{CD}_3)_2\text{SO}$) δ 151.99, 147.09, 145.59, 135.00, 133.75, 130.70, 130.12, 129.54, 127.96, 127.60, 127.27, 127.07, 124.70, 122.03, 70.59, 60.04; HRMS (ESI) m/z calcd. for $\text{C}_{16}\text{H}_{13}\text{N}_5\text{O}_5\text{S}$ $[\text{M}]^+$: 387.0637, found: 387.0637; yield: 92%; melting point: 205–208 °C.

2-(((1-(*n*-pentyl)-1H-1,2,3-triazol-4-yl)methoxy)methyl)benzenethiol (**5q**). ^1H NMR (400 MHz, $(\text{CD}_3)_2\text{SO}$) δ 7.99 (1H, s), 7.23 (1H, d, $J = 4.0$ Hz), 7.13–7.06 (3H, m), 4.66 (2H, s), 4.56 (2H, s), 4.20–4.03 (2H, m), 3.56 (1H, s), 1.82–1.78 (2H, m), 1.42–1.34 (4H, m), 1.01–0.97 (3H, m); ^{13}C NMR (101 MHz, $(\text{CD}_3)_2\text{SO}$) δ 142.45, 133.75, 130.12, 129.54, 127.96, 127.27, 127.07, 124.44, 70.59, 60.04, 51.72, 29.80, 26.85, 22.93, 14.01; HRMS (ESI) m/z calcd. for $\text{C}_{15}\text{H}_{21}\text{N}_3\text{OS}$ $[\text{M}]^+$: 291.1405, found: 291.1405; yield: 87%; melting point: 209–211 °C.

2-(((1-(*n*-heptyl)-1H-1,2,3-triazol-4-yl)methoxy)methyl)benzenethiol (**5r**). ^1H NMR (400 MHz, $(\text{CD}_3)_2\text{SO}$) δ 7.99 (1H, s), 7.23–7.06 (4H, m), 4.66 (4H, s), 4.13–4.02 (2H, m), 3.29 (1H, s), 1.82–1.76 (2H, m), 1.36–1.31 (8H, m), 1.09–0.97 (3H, m); ^{13}C NMR (101 MHz, $(\text{CD}_3)_2\text{SO}$) δ 142.45, 133.75, 130.12, 129.54, 127.96, 127.27, 127.07, 124.44, 70.59, 60.04, 51.72, 31.64, 29.06, 27.55, 26.96, 22.93, 14.01; HRMS (ESI) m/z calcd. for $\text{C}_{17}\text{H}_{25}\text{N}_3\text{OS}$ $[\text{M}]^+$: 319.1718, found: 319.1718; yield: 86%; melting point: 214 °C.

2-(((1-(*n*-nonyl)-1H-1,2,3-triazol-4-yl)methoxy)methyl)benzenethiol (**5s**). ^1H NMR (400 MHz, $(\text{CD}_3)_2\text{SO}$) δ 7.99 (1H, s), 7.24–7.26 (1H, m), 7.13–7.07 (3H, m), 5.07 (1H, s), 4.65 (2H, s), 4.56 (2H, s), 4.20–4.01 (2H, m), 1.83–1.79 (2H, m), 1.46–1.31 (12H, m), 1.09–0.97 (3H, m); ^{13}C NMR (101 MHz, $(\text{CD}_3)_2\text{SO}$) δ 142.45, 133.75, 130.12, 129.54, 127.96, 127.27, 127.07, 124.44, 70.59, 60.04, 51.72, 31.64, 29.06, 28.95, 27.55, 26.96, 22.93, 14.01; HRMS (ESI) m/z calcd. for $\text{C}_{19}\text{H}_{29}\text{N}_3\text{OS}$ $[\text{M}]^+$: 347.2031, found: 347.2031; yield: 85%; melting point: 210–212 °C.

2-(((1-(*n*-decyl)-1H-1,2,3-triazol-4-yl)methoxy)methyl)benzenethiol (**5t**). ^1H NMR (400 MHz, $(\text{CD}_3)_2\text{SO}$) δ 7.99 (1H, s), 7.24–7.22 (1H, m), 7.11–7.04 (3H, m), 4.67 (2H, s), 4.65 (2H, s), 4.24–3.95 (2H, m), 3.30 (1H, s), 1.84–1.79 (2H, m), 1.46–1.32 (14H, m), 1.09–0.97 (3H, m); ^{13}C NMR (101 MHz, $(\text{CD}_3)_2\text{SO}$) δ 142.45, 133.75, 130.12, 129.54,

127.96, 127.27, 127.07, 124.44, 70.59, 60.04, 51.72, 31.64, 29.06, 28.95, 27.55, 26.96, 22.93, 14.01; HRMS (ESI) m/z calcd. for $C_{20}H_{31}N_3OS$ $[M]^+$: 361.2188, found: 361.2188; yield: 92%; melting point: 216 °C.

2-(((1-dodecyl-1H-1,2,3-triazol-4-yl)methoxy)methyl)benzenethiol (**5u**). 1H NMR (400 MHz, $(CD_3)_2SO$) δ 7.84 (1H, s), 7.25–7.27 (1H, m), 7.11–7.04 (3H, m), 4.64 (2H, s), 4.60 (2H, s), 4.43 (1H, s), 4.18–3.98 (2H, m), 1.78–1.74 (2H, m), 1.48–1.32 (18H, m), 1.02–0.99 (3H, m); ^{13}C NMR (101 MHz, $(CD_3)_2SO$) δ 142.45, 133.75, 130.12, 129.54, 127.96, 127.27, 127.07, 124.44, 70.59, 60.04, 51.72, 31.64, 29.06, 28.95, 27.55, 26.96, 22.93, 14.01; HRMS (ESI) m/z calcd. for $C_{22}H_{35}N_3OS$ $[M]^+$: 389.2501, found: 389.2501; yield: 91%; melting point: 228 °C.

2.2. Biology

2.2.1. Cell culture

The human ovarian cancer cell lines CAOV3, CAOV4 and ES-2 were obtained from the Shanghai Institute of Biochemistry and Cellular Biology of the Chinese Academy of Sciences (Shanghai, China). Dulbecco's modified Eagle's medium (DMEM; Gibco Life Technologies, Carlsbad, CA, USA) mixed with 10% fetal bovine serum was used for culturing the cell lines. The medium was supplemented with penicillin (100 U/ml) and streptomycin (100 U/ml) and the cells were cultured at 37 °C under humidified atmosphere containing 5% CO_2 .

2.2.2. MTT (3-(4,5-Dimethylthiazol-2-yl)-2,5-Diphenyltetrazolium bromide) assay

Changes in proliferation of CAOV3 cells after incubation with compound **5a** were analysed by MTT assay [20]. Briefly, CAOV3 cells were dispersed at 1.5×10^6 cells/ml density into the 96-well plates. The cells were subjected to incubation with 0.25, 0.5, 0.75, 1.0, 1.5, 1.75 and 2.0 μM concentrations of compound **5a** for 48 h in an incubator under 5% CO_2 at 37 °C. Following incubation, 20 μl of MTT solution (5 mg/ml) was put into each well of the plate and incubated for 4 h. From each well supernatant was decanted and dimethyl sulfoxide (150 μl) was added. Cell viability was determined by measuring the absorbance of each well at 490 nm. The reading were measured three times for each of the well.

2.2.3. DNA fragmentation assay

Into T-75 flasks, CAOV3 cells were cultured for 12 h at 2×10^5 cells per flask density [25]. The medium was then replaced with fresh medium containing 0.25, 0.5, 1.0, 1.5 and 2.0 μM concentrations of compound **5a** and incubated in it for 48 h. The genomic DNA was prepared using QIAamp DNA Mini kit (Qiagen) according to the guidelines mentioned in the user manual. Agarose gel (1.8%) was used for the DNA sample electrophoresis over 2 h at 50 V. The gels were stained with ethidium bromide (Sigma-Aldrich) and subjected to visualization under ultraviolet (UV) trans-illuminator (Wealtech Corp., Reno, NV, USA).

2.2.4. Cell cycle analysis

In 6-well plates CAOV3 cells at a density of 3×10^6 cells per well were added and cultured for 24 h [25]. The compound **5a** at 0.25, 0.5, 1.0, 1.5 and 2.0 μM concentrations was put into the plates and cells were incubated for 48 h. After compound **5a** treatment the cells were washed with PBS, collected and subjected to overnight fixing in ethyl alcohol (70%) at 4 °C. Then tris-hydrochloride buffer (pH 7.6) mixed with 1% RNase A was added to the cells followed by propidium iodide staining. Cell cycle distribution of CAOV3 cells was assessed by examining the DNA contents using flow cytometry.

2.2.5. Invasion assay

CAOV3 cell invasion potential after incubation with compound **5a**

was assessed by Transwell assay [26]. Briefly, the cells were incubated with 0.25, 0.5, 1.0, 1.5 and 2.0 μM concentrations of compound **5a** for 8 h. The cells following incubation were harvested and subsequently seeded onto the upper chambers at 2×10^5 cells/ml density in the serum-free DMEM. The lower chambers contained DMEM mixed with fetal bovine serum (10%). The cell culture was performed for 24 h and subsequently the chambers were inverted for staining the cells with hematoxylin. The proportion of the cells migrated to lower chamber was calculated for the assessment of invasion potential. The cell counting was carried out randomly in five fields and images were captured at x400 magnification.

2.2.6. Migration assay

CAOV3 cell migration potential after incubation with compound **5a** was determined by wound-healing assay. The cells were incubated with 0.25, 0.5, 1.0, 1.5 and 2.0 μM concentrations of compound **5a** for 48 h at 2×10^5 density per well in 6-well plates [27]. The cells were scratched using plastic scraper and the cellular monolayer was washed to clear it from the detached cells. The adherent cells were subjected to incubation for 24 h under an atmosphere of 5% CO_2 at 37 °C. The migration potential of CAOV3 cells was recorded by monitoring the distance travelled by the cells in the scraped region.

2.2.7. Western blot analysis

CAOV3 cells were subjected incubation with 0.25, 0.5, 1.0, 1.5 and 2.0 μM concentrations of compound **5a** for 48 h. The cells were collected, washed with PBS and subsequently lysed by treatment with RIPA (Roche, Shanghai, China) for 45 min under ice-cold conditions assay [27]. The cellular lysates were subjected to centrifugation for 20 min at 14,000 rpm at 4 °C. The concentration of proteins was analysed by the bicinchoninic acid (BCA) and separation was achieved on SDS-PAGE gel (10%). The proteins were transferred subsequently to polyvinylidene difluoride membranes. Incubation of the membranes was then performed overnight with primary antibodies at 4 °C. After incubation, membranes were washed using tris-buffered saline and Tween-20 three times. Then, the membrane incubation was carried out at room temperature with horseradish peroxidase-labelled goat anti-rabbit IgG secondary antibody for 1 h. Detection of the protein bands was performed using chemiluminescence and autoradiography (ChemiDoc XRS; Bio-Rad Laboratories, Inc., Hercules, CA, USA). The Quantity One software version 4.6.2 (Bio-Rad Laboratories, Inc., Hercules, CA, USA) was used for densitometry determination. The primary antibodies used were against MMP-2 (dilution 1:1000; catalog number #4022), MMP-9 (dilution 1:500; catalog number #3852), p-FAK (dilution 1:500; catalog number #3283), FAK (dilution 1:500; catalog number #3285) and β -actin (dilution 1:1000; catalog number #4967) (Cell Signalling, Shanghai, China).

2.2.8. Animals

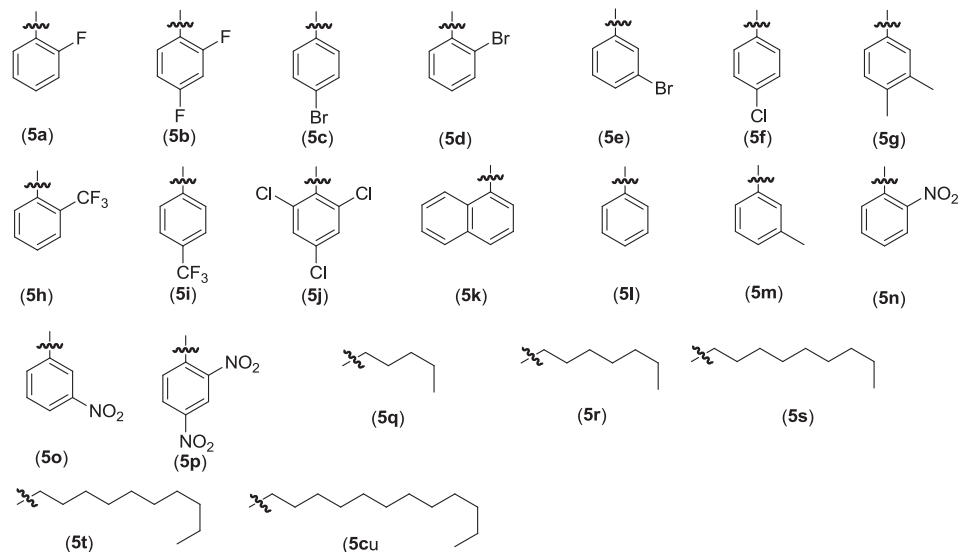
Twenty 5-week old female BALB/c nude mice were purchased from the Chinese Academy of Science. The mice were acclimated one week before the actual experiment to the laboratory conditions and were housed under standard laboratory conditions. All the mice were provided free access to food and water *ad libitum*. The experimental procedures were performed according to the guidelines issued by the Animal Ethics Committee, School of Medicine, Shanghai Jiaotong University, China.

2.2.9. Preparation of ovarian cancer mice model

The solid viable tumor mass was established by inoculation of CAOV3 cells at a concentration of 2×10^6 in 100 μl volume of PBS on the dorsal side of nude mice [28]. From the mice tumor was extracted under anesthesia by laparotomy and then dissected into small pieces

of 1 mm³ dimension. The tumor was implanted into the right ovary of mice orthotopically through surgical suture under sterilized conditions. The ovary was placed to its original site carefully and the wall of abdominal cavity was stitched using 3-0 silk suture. The mice were then assigned randomly into three groups of 5–each. The mice in the two treatment groups were intraperitoneally administered compound **5a** dissolved in DMSO at 5 mg/kg and 10 mg/kg doses after 1 h

synthesized using click chemistry procedure and evaluated against ovarian cancer cells. For this purpose, thiophenol was subjected to MBH-reaction using DABCO (1,4-diazabicyclo[2.2.2]octane) as base to obtain α -hydroxymethyl thiophenol (**3**) in 89% yield. The compound **3** was subsequently propargylated using NaH under anhydrous conditions to afford the alkyne derivative (**4**) in 86% yield (Scheme 1).



of tumor implantation. Mice in the untreated group received equal of normal saline. The mice were sacrificed on day 21 after tumor implantation to extract liver, lungs, intestine and peritoneal tissues for analysis of tumor metastasis. The extracted tumor samples were fixed in formalin (10%) and then embedded in paraffin wax. The tissue samples were sliced into 2 μ m sections and then subjected to H&E for histopathological examination.

2.2.10. Immunohistochemical analysis

The pulmonary, intestinal, peritoneal and liver tissues sections after extraction and PBS washing were embedded in paraffin wax. The samples were cut into thin 2 μ m sections and subjected to incubation with antibodies against vWF (Dako, Australia) [27]. The samples after washing were incubated with horseradish peroxidase (HRP)-conjugated rabbit anti-rat secondary antibody (Dako). The sections were then stained with 3,3'-diaminobenzidine (DAB) and subsequently subjected to hematoxylin counterstaining. The image examination software Image Pro Plus version 4.5 software (Diagnostic Instruments, USA) was used for the immunohistochemical quantification of the digitized images.

2.2.11. Statistical analysis

All the experiments were repeated three times. The data presented are the means \pm standard SD. Student's *t*-test and one-way ANOVA were used for the data analysis. The $P < 0.05$ was taken to indicate statistically significant differences. SPSS v17 software (SPSS, Inc., Chicago, IL, USA) was used for statistical analysis of the data.

3. Results and discussion

3.1. Chemistry

Considering the biological importance of triazolyl derivatives, a series of thiophenol-formaldehyde-triazolyl (TFT) compounds was

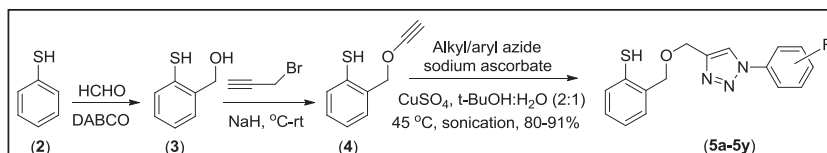
The aromatic azides required were synthesized from the anilines by diazotization reaction with sodium nitrite under acidic conditions and subsequently reacted in situ with sodium azide (Scheme 2).

All the aliphatic azides were synthesized by the reaction of aliphatic alcohol with NaN₃, Ph₃P and I₂ in the presence of imidazole as base (Scheme 3).

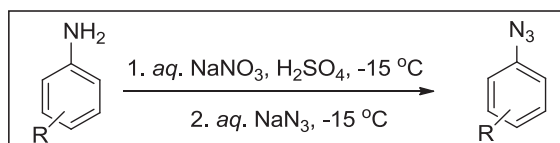
The alkyne derivative (**4**) was subjected to 1,3-dipolar cycloaddition reaction with the synthesized aromatic and aliphatic azides. The reaction was performed using CuSO₄·5H₂O and sodium ascorbate in the presence of *t*-BuOH/H₂O (2:1; v/v) solvent (Scheme 1). The reaction lead to the formation of 1,4-substituted-triazole compounds (**5a–5u**) in very good yield under sonication at a temperature of 45 °C in 1–2 h (Scheme 1). The products obtained were characterized by ¹H NMR, ¹³C NMR, and HRMS techniques. In ¹H NMR, cyclization of azides to form triazoles was confirmed by the resonance of H-atom of triazole ring at δ 8.0 Hz in addition to, chemical shift of other protons in aromatic and aliphatic region. The structure was further supported by ¹³C NMR and HRMs, which showed all the expected carbon signals corresponding to the triazolyl derivatives.

3.2. Biology

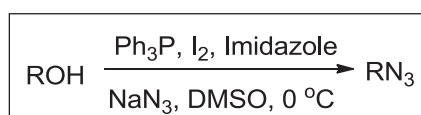
Initial screening of the synthesized compounds (**5a–5u**) against CAOV3, CAOV4 and ES-2 ovarian cancer cells revealed that five-compounds **5a**, **5b**, **5j**, **5h** and **5i** significantly inhibited viability. However, among the five compounds **5a** was found to be most active against the tested ovarian cancer cell lines. The inhibitory effect of compound **5a** on ovarian cancer cells was investigated in detail. Compound **5a** significantly inhibited the viability of CAOV3, CAOV4 and ES-2 cells in a concentration-dependent manner (Fig. 2). The cell viability was measured on treatment with 0.25, 0.5, 0.75, 1.0, 1.5, 1.75 and 2.0 μ M concentrations of compound **5a**. The



Scheme 1. Synthesis of thiophenol-formaldehyde-triazolyl (TFT) compounds. Library of the synthesized compounds. Isolated yield of the compounds 86–94%.



Scheme 2. Preparation of aromatic triazoles.



Scheme 3. Preparation of aliphatic triazoles.

viability was reduced significantly ($P < 0.05$) at 48 h on treatment with compound **5a** from 0.5 μM concentration. The CAOV3, CAOV4 and ES-2 cell viability was reduced to 27, 26 and 29%, respectively on incubation with 2.0 μM concentration of compound **5a** for 48 h. At 0.25 μM concentration, compound **5a** did not change the viability of CAOV3, CAOV4 and ES-2 cells significantly.

In CAOV3 cells compound **5a** treatment for 48 h was followed by the analysis of cell apoptosis by staining with Hoechst 33342 (Fig. 3). Increase in the compound **5a** concentration from 0.25 to 2.0 μM enhanced apoptotic cell proportion significantly ($P < 0.05$). At 2.0 μM concentration of compound **5a** the presence of characteristic apoptotic nuclei was evident in CAOV3 cell cultures. The apoptotic nuclei were not seen in CAOV3 cells cultured for 48 h in the absence of compound **5a**. The percentage of apoptotic nuclei was recorded as 1.26, 8.67, 21.54, 45.89 and 62.53%, respectively on treatment with 0.25, 0.5, 1.0, 1.5 and 2.0 μM concentrations of compound **5a** for 48 h.

CAOV3 cells after exposure to 0.25, 0.5, 1.0, 1.5 and 2.0 μM concentrations of compound **5a** for 48 h were analysed by flow cytometry (Fig. 4). A significant increase in the percentage of CAOV3 cells was observed in G0/G1 phase on exposure to compound **5a**. The percentage of CAOV3 cells in G2/M and S phases decreased with the increase in concentration of compound **5a**. Exposure to 2.0 μM concentration of compound **5a** increased percentage of CAOV3 cells in G0/G1 to 69.54% in comparison to 57.77%

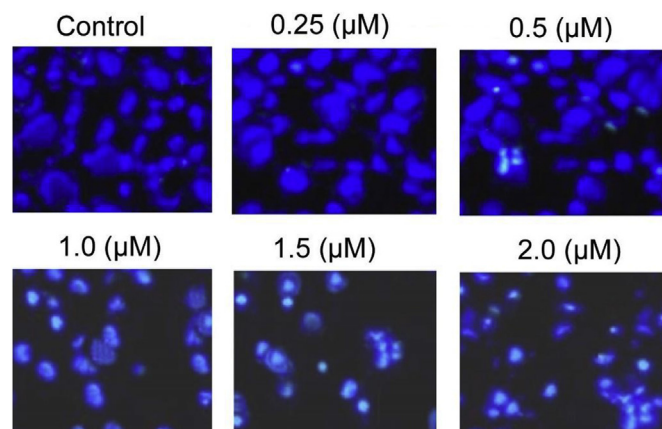


Fig. 3. Compound **5a** treatment leads to nuclear fragmentation in CAOV3 cells. (A) The cells after compound **5a**-treatment were analysed for nuclear morphology using Hoechst 33342 staining by a fluorescent microscope.

in the untreated cells. The population of CAOV3 cells in the S phase decreased to 11.48% on exposure to 2.0 μM concentration of compound **5a** in comparison to 18.89% in control cultures. In G2/M phase compound **5a** exposure at 2.0 μM concentration reduced CAOV3 cell population to 18.08% compared to 22.68% in the untreated cultures.

Carcinoma development and its progression is associated with the invasion and migration potential of the cells [29,30]. Detached cancer cells use the membrane receptors to penetrate different microenvironments for metastasis [29,30]. In the present study the invasive potential of CAOV3 cells was reduced significantly ($P < 0.05$) on treatment with compound **5a** in concentration based manner (Fig. 5). The cells after 48 h of incubation with 0.25, 0.5, 1.0, 1.5 and 2.0 μM concentrations of compound **5a** were examined by Transwell assay. The invasive potential of CAOV3 cells didn't show any significant change on treatment with 0.25 μM concentration of compound **5a**. Incubation with 0.5, 1.0, 1.5 and 2.0 μM concentrations of compound **5a** decreased cell invasion to 84.54, 67.76, 39.14 and 8.62%, respectively.

These findings proved that compound **5a** also inhibits tumor metastasis *in vivo* in mice. To understand the mechanism of

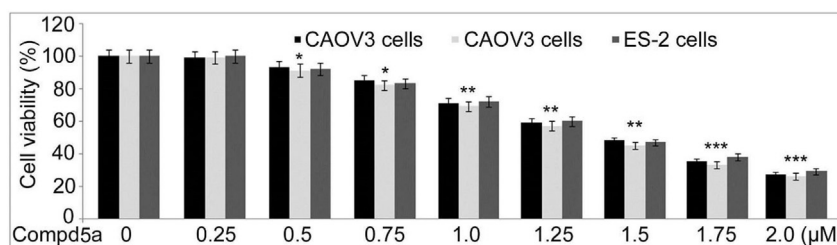


Fig. 2. Effect of compound **5a** on CAOV3, CAOV4 and ES-2 cell viability. The cells were incubated with compound **5a** for 48 h. Viability of the cells was assessed by MTT assay at 48 h * $P < 0.05$, ** $P < 0.02$ and *** $P < 0.01$ compared to 0 μM compound **5a** concentration.

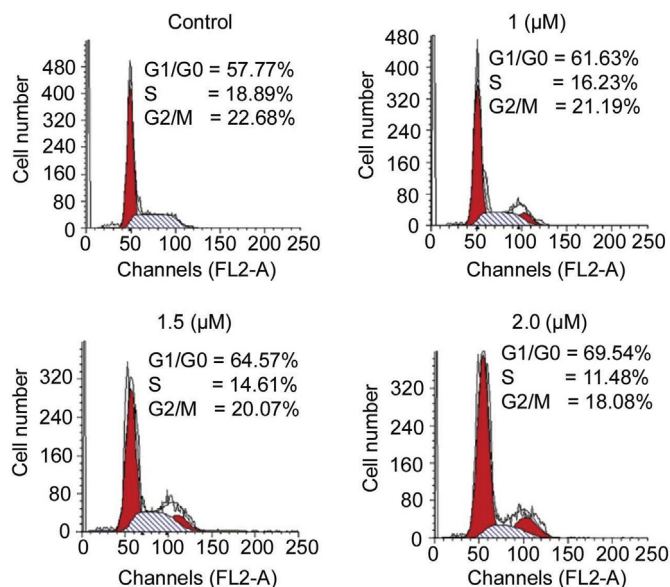


Fig. 4. Cell cycle arrest in CAOV3 cells in G0/G1 phase by compound **5a**. The cells after exposure to compound **5a** were examined by flow cytometry. The presented values are mean \pm SD of three separate experiments.

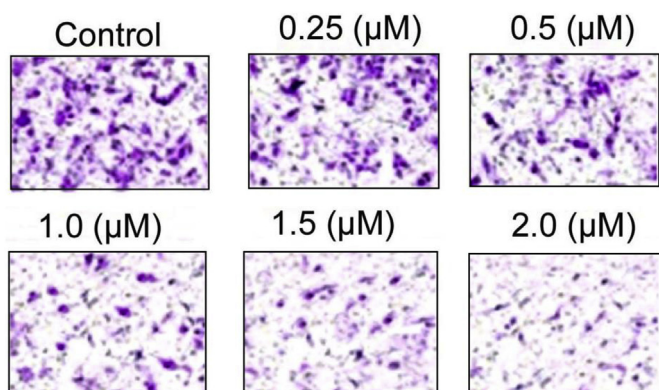


Fig. 5. Effect of compound **5a** on invasion of CAOV3 cells. The cell incubation with compound **5a** was followed by assessment of invasion potential by Transwell method. The images were captured at x100 magnification.

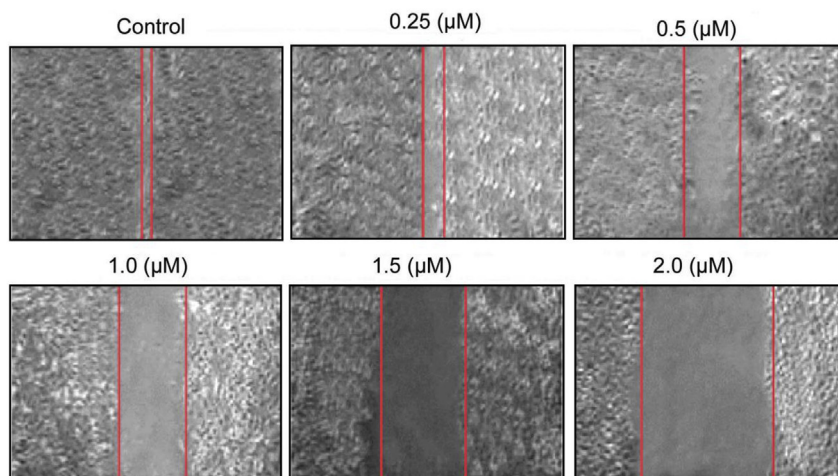


Fig. 6. Effect of compound **5a** on migration of CAOV3 cells. The cell incubation with compound **5a** for 48 h was followed by assessment of migration potential by wound healing assay. The images were captured at x100 magnification.

compound **5a** mediated suppression of tumor metastasis the expression of pathways and molecules associated with the cell invasion and migration was investigated. The cell metastasis is commonly regulated by the matrix metalloproteinases, TIMPs and FAK [31,32]. Activation of FAK plays an important role in the migration and proliferation of tumor cells through alteration of cell-ECM interactions [32,33]. The CAOV3 cell migration after 48 h of treatment with 0.25, 0.5, 1.0, 1.5 and 2.0 μ M concentrations of compound **5a** was determined by wound healing assay (Fig. 6). Increasing the concentration of compound **5a** from 0.5 to 2.0 μ M led to a significant ($P < 0.05$) decrease in the migration potential of CAOV3 cells. The cell migration was decreased from 89.65 to 6.43% with the increase in compound **5a** concentration from 0.5 to 2.0 μ M.

Metastasis of the tumor cells is facilitated by the matrix metalloproteinases through break down of basement membrane and components of extracellular matrix [29,31,34]. The metastasis potential of tumor cells is related to the expression of matrix metalloproteinase-9 [31]. In the present study the effect of 0.25, 0.5,

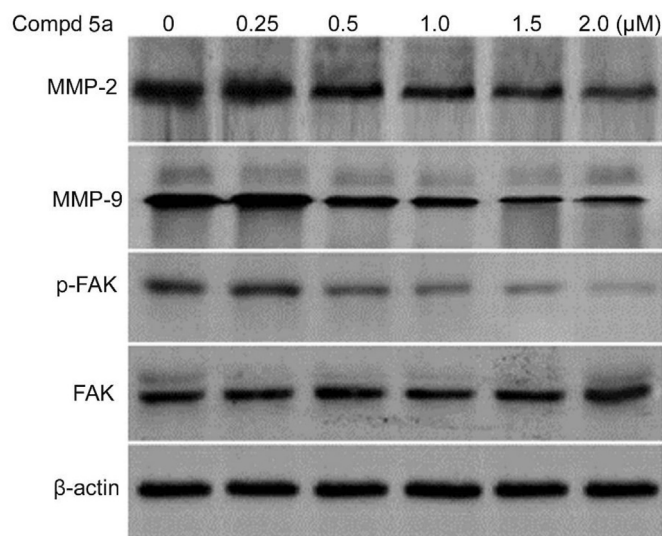


Fig. 7. Effect of compound **5a** on MMPs and FAK expression. The protein expression in CAOV3 cells after incubation with compound **5a** was assessed by western blotting. The protein expression was compared to β -actin as loading control.

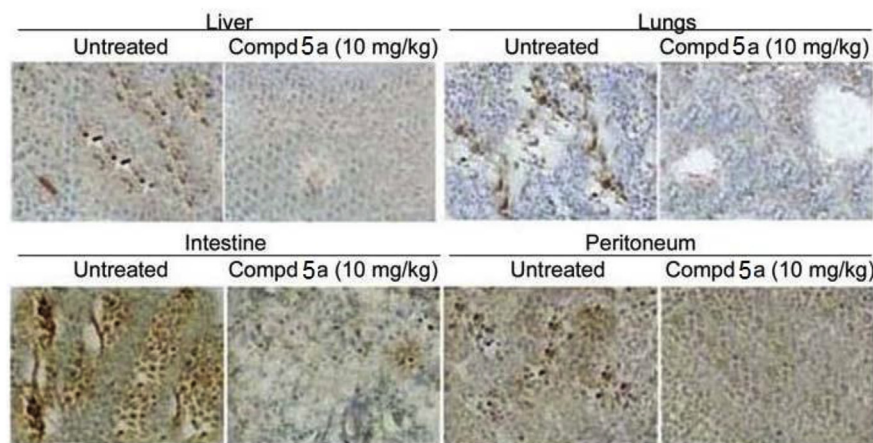


Fig. 8. Compound **5a** inhibits vWF expression in tumor metastasis lesions. The vWF expression was examined in the lesions extracted from liver, lungs, intestinal and peritoneal tissues.

1.0, 1.5 and 2.0 μM concentrations of compound **5a** on the expression of MMP-2 and -9 in CAOV3 cells was determined by Western blot assay (Fig. 7). Compound **5a** treatment markedly decreased the level of MMP-2 and -9 in CAOV3 cells from 0.5 μM concentration. No difference in the MMP-2 and -9 expression in untreated and 0.25 μM compound **5a** treatment CAOV3 cells cultures was recorded. Treatment of CAOV3 cells with compound **5a** caused a marked decrease in FAK activation from 0.5 μM concentration at 48 h. With the enhancement of compound **5a** concentration from 0.5 to 2.0 μM a remarkable decrease was recorded in p-FAK expression.

Metastasis of the malignant tumor cells also depends on the vWF expression which determines neovascularisation [35]. In the tumor microenvironment macrophages promote angiogenesis of the cells by secreting matrix proteases [36,37]. In the ovary tumor mice model effect of compound **5a** on tumor metastasis was analysed after 20 days. The tumor growth was inhibited in the compound **5a** treated mice markedly than those of untreated mice. However, the tumor growth was slightly larger in the 5 mg/kg compound **5a** treatment group than the 10 mg/kg groups. The size of tumor extracted from negative control, untreated, 5 mg/kg and 10 mg/kg compound **5a** treatment groups was measured as 0, 1956 ± 367 , 1258 ± 298 and 213.34 mm^3 , respectively on day 20. Metastasis of tumor was observed to liver, intestine, spleen and peritoneal cavity in all the mice of untreated group. However, the tumor metastasis was decreased in mice treated with 10 mg/kg compound **5a**. Examination of vWF expression by immunohistochemistry in liver, intestinal, pulmonary and peritoneal lesions showed a marked decrease in compound **5a**-treated mice (Fig. 8).

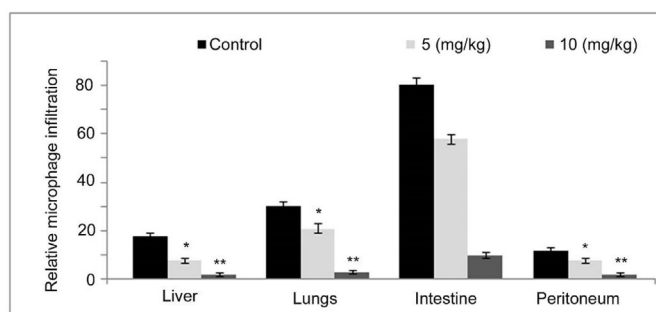


Fig. 9. Compound **5a** suppresses macrophage infiltration into metastatic tumor. Immunohistochemistry was used to determine macrophage infiltration in tumor metastasis lesions from liver, intestinal and pulmonary tissues.

The vWF expression was reduced to ~7, ~8, 6, and ~5%, respectively in liver, lungs, intestinal and peritoneal lesions of 10 mg/kg treatment group compared to the untreated mice. In the 5 mg/kg treatment group the vWF expression was higher than those of 10 mg/kg treatment mice group.

Macrophages also release invasive proteases and adhesion related factors to promote dissemination of the tumors [38,39]. The infiltration of macrophages in the metastatic lesions of liver, intestinal and pulmonary tissues showed a significant decrease in the compound **5a**-treated mice compared to the corresponding lesion from untreated mice (Fig. 9). The suppression of macrophage infiltration was markedly higher in the mice treated with 10 mg/kg doses of compound **5a** compared to 5 mg/kg treatment group. The macrophage infiltration in the lesions of liver, pulmonary tissues intestinal and peritoneum was ~8, ~9, ~7 and ~5% in mice treated with 10 mg/kg doses of compound **5a**.

4. Conclusion

In summary, compound **5a** inhibited ovarian cancer cell proliferation, caused onset of apoptosis and decreased metastasis partly through targeting FAK activation and down-regulation of MMP expression. *In vivo* compound **5a** suppressed tumor development and metastasis by suppression of macrophage infiltration and vWF expression. Thus, compound **5a** needs to be investigated further for the development of ovarian cancer treatment.

Acknowledgements

This study was supported by the Natural science Fund of Science and Technology Department in Jilin (No. 20180101010JC).

Appendix A. Supplementary data

Supplementary data to this article can be found online at <https://doi.org/10.1016/j.ejmech.2019.03.033>.

References

- [1] A. Jemal, R. Siegel, E. Ward, Y. Hao, J. Xu, T. Murray, M.J. Thun, *Cancer statistics*, *CA Cancer J. Clin.* 58 (2008) 71–96.
- [2] M. Raki, D.T. Rein, A. Kanerva, A. Hemminki, *Gene transfer approaches for gynecological diseases*, *Mol. Ther.* 14 (2006) 154–163.
- [3] E.R. Bertone-Johnson, *Epidemiology of ovarian cancer: a status report*, *Lancet* 365 (2005) 101–102.
- [4] A. Jemal, R. Siegel, E. Ward, Y. Hao, J. Xu, M.J. Thun, *Cancer statistics*, 2009, Ca -

- Cancer J. Clin. 59 (2009) 225–249.
- [5] S.I. Kim, J.W. Lee, M. Lee, H.S. Kim, H.H. Chung, J.W. Kim, N.H. Park, Y.S. Song, J.S. Seo, Genomic landscape of ovarian clear cell carcinoma via whole exome sequencing, *Gynecol. Oncol.* 148 (2018) 375–382.
- [6] R. Murakami, N. Matsumura, J.B. Brown, K. Higasa, T. Tsutsumi, M. Kamada, H. Abou-Taleb, Y. Hosoe, S. Kitamura, K. Yamaguchi, et al., Exome sequencing landscape analysis in ovarian clear cell carcinoma shed light on key chromosomal regions and mutation gene networks, *Am. J. Pathol.* 187 (2017) 2246–2258.
- [7] M.K. McConechy, J. Ding, J. Senz, W. Yang, N. Melnyk, A.A. Tone, L.M. Prentice, K.C. Wiegand, J.N. McAlpine, S.P. Shah, et al., Ovarian and endometrial endometrioid carcinomas have distinct CTNNB1 and PTEN mutation profiles, *Mod. Pathol.* 27 (2014) 128–134.
- [8] T. Katoh, M. Yasuda, K. Hasegawa, E. Kozawa, J. Maniwa, H. Sasano, Estrogen-producing endometrioid adenocarcinoma resembling sex cord-stromal tumor of the ovary: a review of four postmenopausal cases, *Diagn. Pathol.* 7 (2012) 164.
- [9] J.K. Sahu, S. Ganguly, A. Kaushik, Triazoles: a valuable insight into recent developments and biological activities, *Chin. J. Nat. Med.* 11 (2013) 456–465.
- [10] M. Olah, R. Rad, L. Ostropovici, A. Bora, N. Hadaruga, D. Hadaruga, R. Moldovan, A. Fulus, M. Mractc, T.I. Oprea, WOMBAT and WOMBAT-PK: bioactivity databases for lead and drug discovery, in: S.L. Schreiber, T.M. Kapoor, G. Wess (Eds.), *Chemical Biology: from Small Molecules to Systems Biology and Drug Design*, vols. 1–3, Wiley-VCH Verlag GmbH, Weinheim, 2008, pp. 760–786.
- [11] X. Li, X.Q. Li, H.M. Liu, X.Z. Zhou, Z.H. Shao, Synthesis and evaluation of antitumor activities of novel chiral 1,2,4-triazole Schiff bases bearing γ -butenolide moiety, *Org. Med. Chem. Lett.* 2 (2012) 26.
- [12] D. Chowrasia, C. Karthikeyan, L. Choure, S. Sahabjada, M. Gupta, M.d. Arshad, P. Trivedi, Synthesis, characterization and anti-cancer activity of some fluorinated 3,6-diaryl-[1,2,4] triazol[3,4-b][1,3,4]thiadiazoles, *Arab. J. Chem* (2013) 6–10.
- [13] P. Chand, J.A. Chesney, B.F. Clem, G.H. Tapolsky, S. Telang, J.O. Trent, Small-Molecule Choline Kinase Inhibitors as Anti-cancer Therapeutics. Patent: US 2011/0257211 A1.
- [14] Y.P. Hou, J. Sun, Z.H. Pang, P.C. Lv, D.D. Li, L. Yan, H.J. Zhang, E.X. Zheng, J. Zhao, H.L. Zhu, Synthesis and antitumor activity of 1,2,4-triazoles having 1,4-benzodioxan fragment as a novel class of potent methionine aminopeptidase type II inhibitors, *Bioorg. Med. Chem.* 19 (2011) 5948–5954.
- [15] V. Georgiyants, L. Perekhoda, N. Saidov, I. Kadamov, Docking studies and biological evaluation of anti-cancer activity of new 1,2,4-triazole (4h) derivatives, *Scr. Sci. Pharm.* 1 (2014) 46–53.
- [16] B.S. Holla, B.K. Sarojini, B.S. Rao, P.M. Akberali, N.S. Kumari, V. Shetty, Synthesis of some halogen-containing 1,2,4-triazolo-1,3,4-thiadiazines and their antibacterial and anticancer screening studies - part I, *Farmaco* 56 (2001) 565–570.
- [17] D. Gupta, D.K. Jain, Synthesis, antifungal and antibacterial activity of novel 1,2,4-triazole derivatives, *J. Adv. Pharm. Technol. Res.* 6 (2015) 141–146.
- [18] D. Dheer, V. Singh, R. Shankar, Medicinal attributes of 1,2,3-triazoles: current developments, *Bioorg. Chem.* 71 (2017) 30–54.
- [19] K. Odlo, J. Hentzen, J.F.D. Chabert, S. Ducki, O.A.B.S.M. Gani, I. Sylte, M. Skrede, V.N. Florenes, T.V. Hansen, 1,5-Disubstituted 1,2,3-triazoles as cis-restricted analogues of combretastatin A-4: synthesis, molecular modeling and evaluation as cytotoxic agents and inhibitors of tubulin, *Bioorg. Med. Chem.* 16 (2008) 4829–4838.
- [20] N. Ashwini, M. Garg, C.D. Mohan, J.E. Fuchs, S. Rangappa, S. Anusha, T.R. Swaroop, K.S. Rakesh, D. Kanojia, V. Madan, A. Bender, H.P. Koeffler, Basappa, B.K.S. Rangappa, Synthesis of 1,2-benzisoxazole tethered 1,2,3-triazoles that exhibit anticancer activity in acute myeloid leukemia cell lines by inhibiting histone deacetylases, and inducing p21 and tubulin acetylation, *Bioorg. Med. Chem.* 23 (2015) 6157–6165.
- [21] S.N.P. Bathula, R. Vadla, Bioactivity of 1,4-disubstituted 1,2,3-triazoles as cytotoxic agents against the various human cell lines, *Asian J. Pharm. Clin. Res.* 4 (2011) 66–67.
- [22] N. Pokhodylo, O. Shyyka, V. Matiychuk, Synthesis of 1,2,3-triazole derivatives and evaluation of their anticancer activity, *Sci. Pharm.* 81 (2013) 663–676.
- [23] R. Majeed, P.L. Sangwan, P.K. Chinthakindi, I. Khan, N.A. Dangroo, N. Thota, A. Hamid, P.R. Sharma, A.K. Saxena, S. Koul, Synthesis of 3-O-propargylated betulinic acid and its 1,2,3-triazoles as potential apoptotic agents, *Eur. J. Med. Chem.* 63 (2013) 782–792.
- [24] S.G. Agalave, S.R. Maujan, V.S. Pore, Click chemistry: 1,2,3-triazoles as pharmacophores, *Chem. Asian J.* 6 (2011) 2696–2718.
- [25] J. Hwang-B, J.H. Park, I.S. Chung, Tumor necrosis factor- α induces apoptosis mediated by Fas signaling pathway in oral squamous cell carcinoma SCC-VII cells, *Oncol. Lett.* 10 (2015) 1016–1022.
- [26] B. Wu, K. Hu, S. Li, J. Zhu, L. Gu, H. Shen, B.D. Hambly, S. Bao, W. Di, Dihydroartemisinin inhibits the growth and metastasis of epithelial ovarian cancer, *Oncol. Rep.* 27 (2012) 101–108.
- [27] H.-Q. Huang, J. Tang, S.-T. Zhou, T. Yi, H.-L. Peng, G.-B. Shen, N. Xie, K. Huang, T. Yang, J.-H. Wu, C.-H. Huang, Y.-Q. Wei, X. Zhao, Orlistat, a novel potent antitumor agent for ovarian cancer: proteomic analysis of ovarian cancer cells treated with Orlistat, *Int. J. Oncol.* 41 (2012) 523–532.
- [28] B. Wu, K. Hui, S. Li, J. Zhu, L. Gu, H. Shen, B.D. Hambly, S. Bao, W. Di, Dihydroartemisinin inhibits the growth and metastasis of epithelial ovarian cancer, *Oncol. Rep.* 27 (2012) 101–108.
- [29] J. Zhang, B. Wang, Arsenic trioxide (As₂O₃) inhibits peritoneal invasion of ovarian carcinoma cells in vitro and in vivo, *Gynecol. Oncol.* 103 (2006) 199–206.
- [30] S. Cattaruzza, R. Perris, Proteoglycan control of cell movement during wound healing and cancer spreading, *Matrix Biol.* 24 (2005) 400–417.
- [31] R. Hoekstra, F.A. Eskens, J. Verweij, Matrix metalloproteinase inhibitors: current developments and future perspectives, *Oncol.* 6 (2001) 415–427.
- [32] J.T. Parsons, K.H. Martin, J.K. Slack, J.M. Taylor, S.A. Weed, Focal adhesion kinase: a regulator of focal adhesion dynamics and cell movement, *Oncogene* 19 (2000) 5606–5613.
- [33] P.P. Provenzano, P.J. Keely, The role of focal adhesion kinase in tumor initiation and progression, *Cell Adhes. Migrat.* 3 (2009) 347–350.
- [34] L. Anfosso, T. Efferth, A. Albin, U. Pfeffer, Microarray expression profiles of angiogenesis-related genes predict tumor cell response to artemisinins, *Pharmacogenomics* 6 (2006) 269–278.
- [35] N. Weidner, J. Folkman, F. Pozza, et al., Tumor angiogenesis: a new significant and independent prognostic indicator in early-stage breast carcinoma, *J. Natl. Cancer Inst.* 84 (1992) 1875–1887.
- [36] L.M. Coussens, Z. Werb, Inflammation and cancer, *Nature* 420 (2002) 860–867.
- [37] C.E. Lewis, J.W. Pollard, Distinct role of macrophages in different tumor microenvironments, *Cancer Res.* 66 (2006) 605–612.
- [38] N. Jonjic, G. Peri, S. Bernasconi, et al., Expression of adhesion molecules and chemotactic cytokines in cultured human mesothelial cells, *J. Exp. Med.* 176 (1992) 1165–1174.
- [39] E. Wang, Y. Ngalame, M.C. Panelli, et al., Peritoneal and subperitoneal stroma may facilitate regional spread of ovarian cancer, *Clin. Cancer Res.* 11 (2005) 113–122.